

# Low-Frequency Magnetic Noise in Statically-Driven Solenoid for Biasing Magnetic Field Sensors

Phillip Durdaut, Henrik Wolframm, and Michael Höft

**Abstract**—For the generation of static magnetic fields solenoids are frequently used for the purpose of research and development of magnetic field sensors. When such a sensor is to be analyzed with regard to its inherent noise the influence of other noise sources of the measurement system needs to be minimized. This article reports on the low-frequency magnetic noise within such a coil system. On the one hand, the impact of the intrinsic noise of the coil itself and on the other hand the impact of additional current noise of various commercially available current sources, which accordingly also leads to magnetic noise within the coil, are investigated. With low-frequency values in the range of a few tens of  $fT/\sqrt{Hz}$ , the coil's inherent noise is mostly neglectable. However, frequently utilized current sources for the generation of a static magnetic bias field lead to significant low-frequency magnetic flux noise typically in the  $nT/\sqrt{Hz}$  regime. It is found that this noise cannot be decreased by increasing the coil's magnetic sensitivity, i.e. the magnetic flux density as a function of the static current. Instead, current sources with very high current-to-current-noise ratios are required.

## I. INTRODUCTION

Similar to biasing bipolar [1, pp. 83-88] or field-effect transistors [1, p. 149] by static currents and voltages, respectively, various types of magnetic field sensors also require a magnetic biasing for maximizing their sensitivity, e.g. sensors based on the magnetostrictive effect. For practical applications, a suitable operating point can be realized via magnetostrictive multilayers, i.e. an exchange bias system [2]. For the purpose of research and development electromagnets are generally used to determine field-dependent properties of a sensor. With regard to the characterization of signal properties or sensitivities coils are generally well suited. However, if the intrinsic noise of a magnetic field sensor is to be determined as a function of an external and static magnetic field, see e.g. [3], the influence of other noise sources of the measurement system needs to be minimized or reduced below the inherent noise of the sensor, respectively. State-of-the-art magnetic field sensors, e.g. sensors based on the  $\Delta E$  effect, currently reach inherent noise levels as low as e.g.  $70 \text{ pT}/\sqrt{Hz}$  at a frequency of 10 Hz [4]. Thus, the additional magnetic noise of the biasing coil system needs to be distinctly smaller than this value, e.g.  $1 \text{ pT}/\sqrt{Hz}$  at a frequency of 10 Hz. Apart from certainly existing exceptions, the frequency range of interest is approximately from 1 Hz (often also below) to 1 kHz.

This article reports on the low-frequency magnetic noise inside such a coil system. All investigations were carried out on a specific coil, the structure of which is explained below.

P. Durdaut, H. Wolframm, and M. Höft are with the Chair of Microwave Engineering, Institute of Electrical Engineering and Information Technology, Faculty of Engineering, Kiel University, Kaiserstr. 2, 24143 Kiel, Germany.

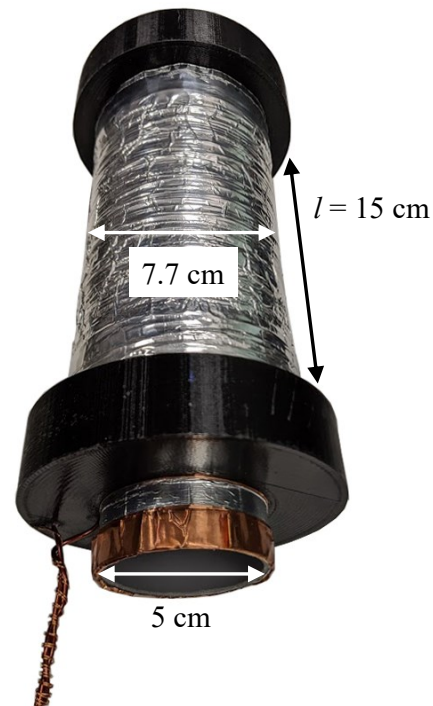


Fig. 1: Photography of the coil system under investigation consisting of two coils wound on top of each other. The inner coil (*DC coil*) is used for generating static bias magnetic fields and the additional outer coil (*AC coil*) enables the generation of dynamic magnetic test signals.

Two different noise sources are considered. On the one hand, the impact of the intrinsic noise of the coil itself and on the other hand the impact of additional current noise of various commercially available current sources, which accordingly also leads to magnetic noise within the coil, are investigated.

## II. COIL SYSTEM

The coil system under investigation of which a photography is shown in Fig. 1 consists of two cylindrical coils, i.e. two solenoids, which are wound on top of each other. The reason for the requirement of two coils is that in measurements for the characterization of magnetic field sensors typically not only a coil for the static bias field is needed, in the following referred to as *DC coil*, but also an additional coil for the generation of dynamic test fields is required, in the following referred to as *AC coil*.

Both coils are wound on a DN 40 plastic pipe with an outer diameter of 5 cm. By means of two 3D printed stoppers

TABLE I: Overview of all relevant parameters of the investigated coil system.

Parameter	Symbol	Inner coil (DC coil)	Outer coil (AC coil)
Coil length	$l$	15 cm	15 cm
Number of turns	$N$	8 x 90 = 720	2 x 300 = 600
Wire diameter	$d_w$	1.5 mm	0.4 mm
Inner diameter	$d_i$	5 cm	4.5 cm
Outer diameter	$d_o$	7.4 cm	7.7 cm
Effective diameter	$d_{\text{eff}} = d_i + (d_o - d_i)/2$	6.2 cm	7.6 cm
Cross-section area	$A = \pi \cdot (d_{\text{eff}}/2)^2$	30.2 cm <sup>2</sup>	45.4 cm <sup>2</sup>
Coil sensitivity	$S = \mu_0 N/l$	6.03 mT/A	5.03 mT/A
		5.95 mT/A (measured)	5.06 mT/A (measured)
Coil inductance	$L = \mu_0 N^2 A/l$	13.1 mH	13.7 mH
		10.4 mH (measured)	10.2 mH (measured)
Coil capacitance	$C$	770 pF (measured)	980 pF (measured)
Parallel resonance frequency	$f_{\text{res}} = 1/(2\pi\sqrt{LC})$	56.2 kHz (measured)	50.3 kHz (measured)
Wire length	$l_w = N\pi d_{\text{eff}}$	140 m	143 m
Wire resistance per meter	$r_w$	21.8 mΩ/m	136 mΩ/m
Wire resistance	$R_w = r_w l_w$	3.1 Ω	19.5 Ω
		1.43 Ω (measured)	19.28 Ω (measured)
Proximity effect loss resistance	$R_p$	550 Ω (measured)	1.8 kΩ (measured)
Intrinsic magnetic noise ( $f < 1$ kHz)	$B_n$	32 fT/ $\sqrt{\text{Hz}}$	15 fT/ $\sqrt{\text{Hz}}$

(black) with a diameter of 10 cm the coil system directly fits into an ultra high magnetic field shielding mu-metal cylinder ZGI from Aaronia AG in which all magnetic measurements are typically performed. The inner distance between the two stoppers yields the length of both coils of  $l = 15$  cm. The inner coil (DC coil) consists of 8 layers of 90 windings each, resulting in a total number of turns of  $N = 720$ . The copper wire itself has a diameter of  $d_w = 1.5$  mm (manufacturer: Elosal). The outer coil (AC coil) consists of 2 layers of 300 windings each, resulting in a total number of turns of  $N = 600$ . The utilized copper wire has a diameter of  $d_w = 0.4$  mm (manufacturer: RS PRO). All relevant parameters of the two coils, some of which will be introduced and further explained below, are summarized in Tab. I.

### III. MAGNETIC SENSITIVITY

One of the most important properties of the coils is their magnetic sensitivity, i.e. the generated homogenous magnetic flux density  $B$  as a function of the current through the coil  $I$ . For a cylindrical and long air coil (relative permeability  $\mu_r = 1$ ) without any ferromagnetic core, the sensitivity

$$S = \frac{B}{I} = \frac{\mu_0 N}{l} \quad (1)$$

can be calculated based on the coil's total number of turns  $N$  and its length  $l$  [5, p. 939]. The additional term  $\mu_0$  represents the vacuum permeability ( $\mu_0 = 4\pi \cdot 10^{-7}$  Vs/Am). With Eq. (1) values of 6.03 mT/A (DC coil) and 5.03 mT/A (AC coil) result.

Both sensitivity values were confirmed by measuring the magnetic flux density  $B$  inside the coils utilizing an FM 302 teslameter (uniaxial probe AS-LAP) from Projekt Elektronik GmbH connected to a lock-in amplifier SR830 from Stanford Research Systems for each coil being fed by a Keithley 6221 current source with an alternating current of an amplitude

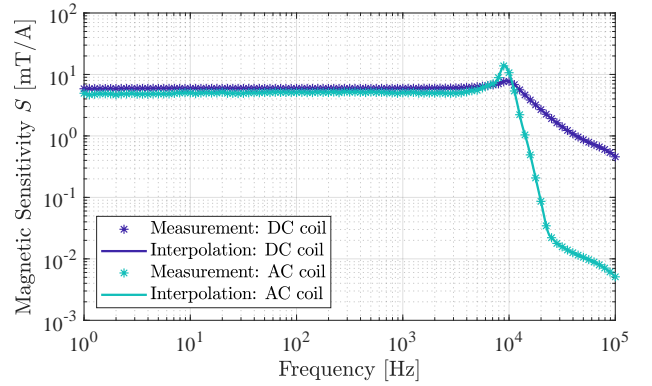


Fig. 2: Measured sensitivities of the two coils as a function of the frequency revealing constant values of 5.95 mT/A (DC coil) and 5.06 mT/A (AC coil) for frequencies below several kilohertz.

of  $\hat{I} = \sqrt{2} I = 100$  mA. The results are shown in Fig. 2 and reveal constant sensitivities of 5.95 mT/A (DC coil) and 5.06 mT/A (AC coil) for frequencies below several kilohertz. At higher frequencies above the inductor's parallel resonance frequency the coils no longer behave inductive but capacitive [6, p. 15] (see the following section) leading to decreasing sensitivities.

### IV. ELECTRICAL IMPEDANCE

The electrical impedance  $Z_{\text{coil}} = R_{\text{coil}} + jX_{\text{coil}}$  of a coil is frequently described by an equivalent circuit as depicted in Fig. 3 [6, pp. 15-20]. In this circuit,  $L$  is the coil's inductance which can be calculated by

$$L = \frac{\mu_0 N^2 A}{l} \quad (2)$$

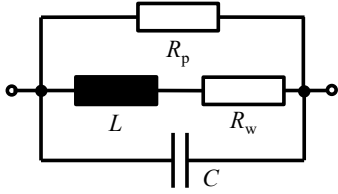


Fig. 3: Equivalent circuit of an air solenoid with the inductance  $L$ , the wire resistance  $R_w$ , and the parasitic capacitance between the windings  $C$ . The parallel resistance  $R_p$  covers for additional loss mechanisms.

where  $A$  is the cross-sectional area of the air solenoid [5, p. 1006]. For the two coils under investigation with parameters as listed in Tab. I, Eq. (2) yields theoretical inductances of 13.1 mH (DC coil) and 13.7 mH (AC coil). Additional parameters of the equivalent circuit are the resistance of the wire  $R_w$ , the parasitic capacitance between the windings  $C$ , and the parallel resistance  $R_p$  covering for additional losses such as losses in the coil's core material (such hysteresis losses do not occur in an air solenoid), losses due to the skin effect, losses due to eddy-currents, and losses due to the proximity effect [7].

The electrical impedance  $Z_{\text{coil}} = R_{\text{coil}} + jX_{\text{coil}}$  of both coils was measured utilizing a calibrated impedance analyzer *Bode 100* from *OMICRON Lab* with the results shown in Fig. 4. For research and development purposes the DC coil is generally used more frequently compared to the AC coil. For this reason and because of the coupling of both coils, the impedance of the DC coil was measured for various cases. As shown in Fig. 4a and Fig. 4b both the real and the imaginary parts slightly depend on the connection state of the AC coil, i.e. whether it is unconnected or connected to a current source (here it is connected exemplary to a frequently utilized current source *Keithley 6221*). However, these differences only occur in the frequency regime of the inductor's parallel resonance. In the practical relevant frequency range below 10 kHz the electrical impedance of the DC coil is not significantly affected by the connection state of the AC coil. Characteristic for the measured impedance curves are the constant real part at low frequencies due to the resistance of the wire ( $R_w$ ) and the parallel resonance frequency [6, p. 16]

$$f_{\text{res}} = \frac{1}{2\pi\sqrt{LC}} \quad (3)$$

at  $f_{\text{res}} = 56.2$  kHz (DC coil) and  $f_{\text{res}} = 50.3$  kHz (AC coil), respectively. In addition, in contrast to an ideal coil, it is noticeable that the real part of the impedance increases with higher frequencies. These losses are attributed to the proximity effect and can be calculated using the *Dowell* model [8].

Based on the measurements of the electrical impedances all parameters of the equivalent circuit (Fig. 3) can be determined, yielding values of  $L = 10.4$  mH,  $R_w = 1.43 \Omega$ ,  $C = 770$  pF, and  $R_p = 550 \Omega$  (DC coil) and  $L = 10.2$  mH,  $R_w = 19.28 \Omega$ ,  $C = 980$  pF, and  $R_p = 1.8$  k $\Omega$  (AC coil). As shown in Fig. 4, both coils are sufficiently described by the equivalent circuit (red dashed lines) in the low-frequency range below 10 kHz.

In fact, for this frequency range, the capacitor can even be neglected ( $C = 0$ , black dashed lines).

## V. MAGNETIC NOISE DUE TO COILS INTRINSIC NOISE

According to the fluctuation–dissipation theorem (FDT) every loss mechanism corresponds with fluctuations. In the particular case of a loss-representing electrical resistance the FDT simplifies to the well-known *Johnson–Nyquist* theorem [9], [10] that relates the voltage fluctuations, i.e. the voltage noise density  $V_n = \sqrt{4k_B T R}$  across the resistance  $R$  with the temperature  $T$  (in the following room temperature with  $T = 290$  K). The term  $k_B$  represents the *Boltzmann* constant.

The coils under investigation exhibit two loss mechanisms as discussed above which are considered by the two resistances  $R_w$  and  $R_p$  in the equivalent circuit (Fig. 3). Accordingly, there are also two voltage noise sources which can be described by the voltage noise densities

$$V_{\text{nw}} = \sqrt{4k_B T R_w} \quad (4)$$

and

$$V_{\text{np}} = \sqrt{4k_B T R_p}. \quad (5)$$

As shown above, the capacitance  $C$  of the equivalent circuit can be neglected in the relevant frequency regime below 10 kHz. Thus, based on the superposition principle, two simple expressions for the corresponding current noise densities through the coil can be derived that are given by

$$I_{\text{nw}} = \frac{V_{\text{nw}}}{|R_w + R_p + j\omega L|} = \sqrt{\frac{4k_B T R_w}{(R_w + R_p)^2 + (\omega L)^2}} \quad (6)$$

and

$$I_{\text{np}} = \frac{V_{\text{np}}}{|R_w + R_p + j\omega L|} = \sqrt{\frac{4k_B T R_p}{(R_w + R_p)^2 + (\omega L)^2}}. \quad (7)$$

With the magnetic sensitivity  $S$ , which relates a current through the coil with a magnetic flux density within the coil, the magnetic flux noise density is given by

$$B_n = S \cdot \sqrt{I_{\text{nw}}^2 + I_{\text{np}}^2} \quad (8)$$

$$= S \cdot \sqrt{\frac{4k_B T (R_w + R_p)}{(R_w + R_p)^2 + (\omega L)^2}} \quad (9)$$

when the two noise sources are assumed as statistically independent. Thus, the noise increases proportionally with the sensitivity of the coil. With the (measured) values as listed in Tab. I virtually frequency-independent values as low as  $B_n^{(\text{DC coil})} = 32$  fT/ $\sqrt{\text{Hz}}$  and  $B_n^{(\text{AC coil})} = 15$  fT/ $\sqrt{\text{Hz}}$  result (dashed and dotted lines in Fig. 5). Due to the rigid connection of both coils, these values cannot be verified separately. Instead, only the sum of the noise contributions of both coils

$$B_n^{\text{total}} = \sqrt{\left(B_n^{(\text{DC coil})}\right)^2 + \left(B_n^{(\text{AC coil})}\right)^2} \quad (10)$$

can be measured, whereby it can be assumed that both noise contributions are statistically independent of each other. Based

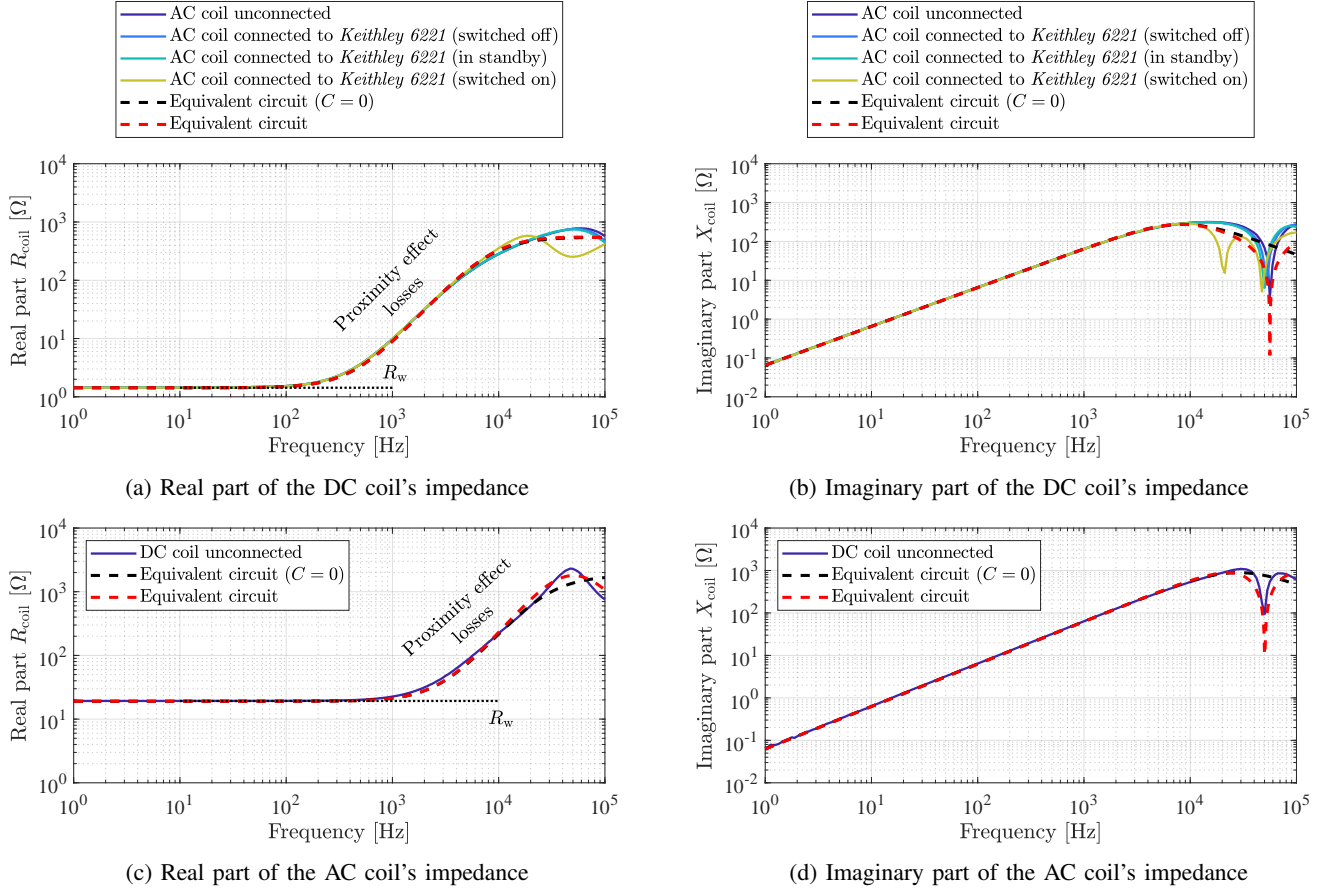


Fig. 4: Measured real (left) and imaginary (right) parts of the DC (top) and AC coil (bottom) from which the parameters of the equivalent circuit (Fig. 3) are extracted as summarized in Tab. I. The DC coil was characterized for several connection states of the AC coil revealing that the relevant low-frequency behavior below 10 kHz is not affected by the AC coil's connection state.

on Eq. (10), a total magnetic flux noise density as low as  $35 \text{ fT}/\sqrt{\text{Hz}}$  can be expected (black solid line in Fig. 5).

To verify this value, two magnetic noise measurements were performed with an optically pumped magnetometer (*QZFM* from *QuSpin* with a bandwidth of 100 Hz) inside a magnetic shielding chamber (*Vacuumschmelze GmbH & Co. KG*, [11, p. 117]). The measurement results are shown in Fig. 5 and basically confirm a magnetic flux noise density within the unconnected coil of several tens of  $\text{fT}/\sqrt{\text{Hz}}$  (red solid line) in the frequency range between 10 Hz and 100 Hz. It is true that the measured values are slightly increased compared to the previously calculated noise. However, the increase in the noise level compared to a reference measurement outside the coil (gray solid line) is clearly visible. In addition, the intrinsic noise of the utilized OPM is also in the range of about  $10 \text{ fT}/\sqrt{\text{Hz}}$ , which also affects the result of the noise measurement within the coil. Below 10 Hz the inherent noise of the sensor and additional disturbances are even higher. Nevertheless, these results can be regarded as verification of the noise calculation and show in particular that the inherent magnetic noise of such a coil is largely negligible, at least when utilized with sensors based on the magnetostrictive effect.

## VI. MAGNETIC NOISE DUE TO CURRENT NOISE OF EXTRINSIC CURRENT SOURCES

The inherent noise of the coil with low-frequency values in the range of a few tens of  $\text{fT}/\sqrt{\text{Hz}}$  has turned out to be very low, i.e. in the same order of magnitude as the inherent noise level of state-of-the-art optically pumped magnetometers. If the coil is fed by an external current source to generate magnetic fields, it must be assumed that additional noise will occur. In the following, the additional noise of several commercial sources is characterized. However, since sensitive magnetic field sensors are generally saturated by the generated magnetic fields, the characterization is performed electrically instead.

For these characterizations, the magnetically shielded DC coil is supplied with relatively high currents while the voltage noise density across the DC coil  $V_n$  is measured with a dynamic signal analyzer *SR785* from *Stanford Research Systems*. With the previously determined electrical impedance of the coil, both the current noise density through the coil

$$I_n = \frac{V_n}{|Z_{\text{coil}}|} \quad (11)$$

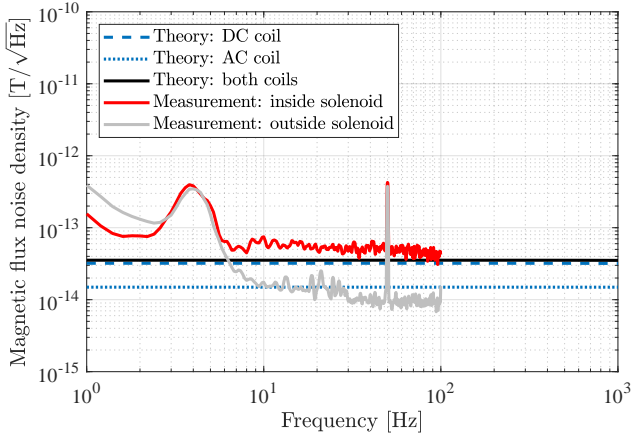


Fig. 5: Calculated and measured magnetic flux noise density inside the solenoid. The measurements were performed with an optically pumped magnetometer and confirm the increased noise floor within the unconnected coil (red solid line) in comparison to a reference measurement outside the coil (gray solid line). Under the given circumstances that the detectivity of the utilized sensor is only slightly below the inherent noise of the coil and impairs the measurement accordingly, the measurement results can be regarded as verification of the model calculations.

and the magnetic flux noise density within the coil

$$B_n = S \cdot I_n = S \cdot \frac{V_n}{|Z_{\text{coil}}|} \quad (12)$$

can be calculated, where the sensitivity  $S$  is again utilized for the conversion between current and magnetic flux density. As before, the magnetic noise is directly proportional to the magnetic sensitivity of the coil. The results shown in Fig. 6 reveal a significant increase in magnetic flux noise to values, depending on the frequency, in the  $\text{nT}/\sqrt{\text{Hz}}$  regime if the coil is fed with a relatively high current of 1 A. Only in case the coil is fed by a *Keithley 6221* current source whose output current is limited to 100 mA the noise floor is in the range of some tens of  $\text{pT}/\sqrt{\text{Hz}}$ . Although it can be seen that its noise increases with low frequencies, this is due to the noise limit of the measurement system, i.e. the inherent noise of the signal analyzer (black line).

## VII. ANALYSIS & CONCLUSION

We reported on the equivalent magnetic flux noise density within a pair of two coils that are typically used for the purpose of research and development of magnetic field sensors, e.g. sensors based on the magnetostrictive effect. Besides an analysis of the magnetic sensitivity and the electrical impedance of both coils, the focus was on the investigation of the coils noise behavior. Based on the losses within the coil, which are taken into account by corresponding resistors in the equivalent circuit, the inherent noise of the coil could be calculated and metrologically verified. In the low-frequency range, however, this magnetic flux density is only in the range of a few tens of  $\text{fT}/\sqrt{\text{Hz}}$ .

The DC coil is used for research and development purposes to generate static bias flux densities  $B$ , typically requiring values up to  $B = 5 \text{ mT}$  depending on the magnetic material [12]. With a sensitivity of the investigated coil of  $S = 5.95 \text{ mT/A}$  this value corresponds with a current of  $I = 0.84 \text{ A}$ . However, measurements have shown that the additional current noise  $I_n$  of commercial current sources then leads to a significant increase of the magnetic flux noise density  $B_n$  typically in the range of some  $\text{nT}/\sqrt{\text{Hz}}$  (depending on the actual source and the frequency). Such values are obviously too high for application with magnetic field sensors with a low-frequency inherent noise below  $100 \text{ pT}/\sqrt{\text{Hz}}$ .

In addition, it has been shown that a *Keithley 6221* current source with a maximum current of  $I = 100 \text{ mA}$  results in a significant lower magnetic flux noise density. Apart from the fact that the resulting noise is still well above  $B_n = 10 \text{ pT}/\sqrt{\text{Hz}}$ , one could come up with the idea to increase the magnetic sensitivity  $S$  to solve the problem. This would result in lower current  $I$  to generate a required magnetic bias flux density  $B$ . However, based on Eq. (1) and Eq. (12), the magnetic-flux-density-to-magnetic-flux-noise-density ratio can be expressed as

$$\frac{B}{B_n} = \frac{S \cdot I}{S \cdot I_n} = \frac{I}{I_n} \quad (13)$$

which is obviously independent of the magnetic sensitivity  $S$  and which is only determined by the current-to-current-noise ratio of the current source. For exemplary values of  $B = 5 \text{ mT}$  and  $B_n = 1 \text{ pT}/\sqrt{\text{Hz}}$  a current-to-current-noise ratio of

$$\frac{I}{I_n} = \frac{B}{B_n} = \frac{5 \text{ mT}}{1 \text{ pT}/\sqrt{\text{Hz}}} = 500 \cdot 10^9 \sqrt{\text{Hz}} \quad (14)$$

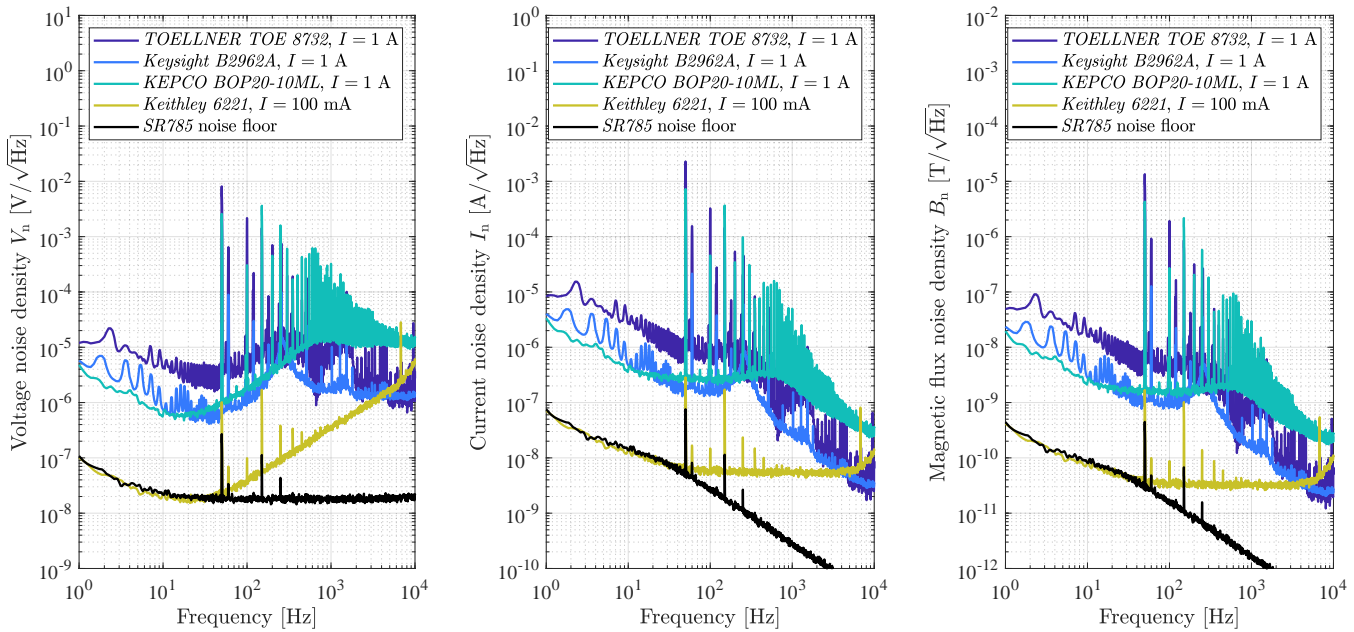
or

$$10 \cdot \log_{10} \left( \frac{\left(\frac{I}{I_n}\right)^2}{1 \text{ Hz}} \right) \text{ dBHz} = 194 \text{ dBHz}, \quad (15)$$

respectively, would be required. Although, to the best of our knowledge, no commercial current sources are available that reach that value, literature reports on ultra low-noise semiconductor current sources with achieved values as high as 190 dBHz [13], 135 dBHz [14], 128 dBHz [15], 122 dBHz [16], and 172 dBHz [17], each at a frequency of 1 Hz. In addition, it must be mentioned that these current sources are usually limited to output currents of a few tens of mA, so that a coil with a much higher magnetic sensitivity  $S$  would still be required.

## ACKNOWLEDGMENT

This work was supported by the German Research Foundation (Deutsche Forschungsgemeinschaft, DFG) through the Collaborative Research Centre CRC 1261 *Magnetolectric Sensors: From Composite Materials to Biomagnetic Diagnostics*. In addition, the authors would like to thank Eric Elzenheimer for supporting the magnetic noise measurements with an optically pumped magnetometer.



(a) Voltage noise density across the coil      (b) Current noise density through the coil      (c) Magnetic flux noise density within the coil

Fig. 6: Measurements of the magnetic flux noise density in the DC coil (c), by means of electrical measurements of the voltage noise density across the DC coil (a), and corresponding calculations of the current noise density through the coil (b) for various commercial current sources. The black line represents the noise limit of the measurement system, i.e. the noise floor of the utilized signal analyzer SR785 from *Stanford Research Systems*.

## REFERENCES

- [1] P. Horowitz and W. Hill, *The Art of Electronics*. New York City, New York, USA: Cambridge University Press, 2015.
- [2] E. Lage, C. Kirchhof, V. Hrkac, L. Kienle, R. Jahns, R. Knöchel, E. Quandt, and D. Meyners, "Exchange biasing of magnetoelectric composites," *Nature Materials*, vol. 11, no. 6, pp. 523–529, Jun. 2012.
- [3] P. Durdaut, E. Rubiola, J.-M. Friedt, C. Müller, B. Spetzler, C. Kirchhof, D. Meyners, E. Quandt, F. Faupel, J. McCord, R. Knöchel, and M. Höft, "Phase Sensitivity and Phase Noise of Cantilever-Type Magnetoelastic Sensors Based on the  $\Delta E$  Effect," Preprint arXiv:2003.01085 (physics.ins-det), March 2020.
- [4] V. Schell, C. Müller, P. Durdaut, A. Kittmann, L. Thormählen, F. Lofink, D. Meyners, M. Höft, J. McCord, and E. Quandt, "Magnetic anisotropy controlled FeCoSiB thin films for surface acoustic wave magnetic field sensors," *Applied Physics Letters*, vol. 116, no. 7, pp. 073 503 1–5, Feb. 2020.
- [5] R. A. Serway and J. W. Jewett, *Physics for Scientists and Engineers*, 6th ed. Boston, Massachusetts, USA: Brooks Cole, 2004.
- [6] C. Bowick, *RF circuit design*. Burlington, Massachusetts, USA: Newnes, 1997.
- [7] A. Lotfi, P. Gradzki, and F. Lee, "Proximity effects in coils for high frequency power applications," *IEEE Transactions on Magnetics*, vol. 28, no. 5, pp. 2169–2171, Sep. 1992.
- [8] P. L. Dowell, "Effects of eddy currents in transformer windings," *Proceedings of the Institution of Electrical Engineers*, vol. 113, no. 8, pp. 1387–1394, 1966.
- [9] J. B. Johnson, "Thermal Agitation of Electricity in Conductors," *Physical Review*, vol. 32, no. 1, pp. 97–109, Jul. 1928.
- [10] H. Nyquist, "Thermal Agitation of Electric Charge in Conductors," *Physical Review*, vol. 32, no. 1, pp. 110–113, Jul. 1928.
- [11] R. Jahns, "Untersuchung und Optimierung von Empfindlichkeit und Rauschverhalten magnetoelektrischer Sensoren," Ph.D. dissertation, Kiel University, 2013. [Online]. Available: [https://macau.uni-kiel.de/receive/diss\\_mods\\_00012442](https://macau.uni-kiel.de/receive/diss_mods_00012442)
- [12] X. Liang, C. Dong, H. Chen, J. Wang, Y. Wei, M. Zaeimbashi, Y. He, A. Matyushov, C. Sun, and N. Sun, "A Review of Thin-Film Magnetoelastic Materials for Magnetoelastic Applications," *Sensors*, vol. 20, no. 5, p. 1532, Mar. 2020.
- [13] C. Ciofi, R. Giannetti, V. Dattilo, and B. Neri, "Ultra Low-Noise Current Sources," *IEEE Transactions on Instrumentation and Measurement*, vol. 47, no. 1, pp. 78–81, 1998.
- [14] S. Linzen, T. L. Robertson, T. Hime, B. L. T. Plourde, P. A. Reichardt, and J. Clarke, "Low-noise computer-controlled current source for quantum coherence experiments," *Review of Scientific Instruments*, vol. 75, no. 8, pp. 2541–2544, Aug. 2004.
- [15] C. J. Erickson, M. Van Zijll, G. Doermann, and D. S. Durfee, "An ultrahigh stability, low-noise laser current driver with digital control," *Review of Scientific Instruments*, vol. 79, no. 7, pp. 073 107 1–8, Jul. 2008.
- [16] D. Talukdar, R. K. Chakraborty, S. Bose, and K. K. Bardhan, "Low noise constant current source for bias dependent noise measurements," *Review of Scientific Instruments*, vol. 82, no. 1, pp. 013 906 1–6, Jan. 2011.
- [17] G. Scandurra, G. Cannatà, G. Giusi, and C. Ciofi, "Programmable, very low noise current source," *Review of Scientific Instruments*, vol. 85, no. 12, pp. 125 109 1–10, Dec. 2014.